

# An Accelerated Alternating Partial Bregman Algorithm for ReLU-based Matrix Decomposition

Qingsong Wang\*, Yunfei Qu†, Chunfeng Cui‡, Deren Han§

March 5, 2025

## Abstract

Despite the remarkable success of low-rank estimation in data mining, its effectiveness diminishes when applied to data that inherently lacks low-rank structure. To address this limitation, in this paper, we focus on non-negative sparse matrices and aim to investigate the intrinsic low-rank characteristics of the rectified linear unit (ReLU) activation function. We first propose a novel nonlinear matrix decomposition framework incorporating a comprehensive regularization term designed to simultaneously promote useful structures in clustering and compression tasks, such as low-rankness, sparsity, and non-negativity in the resulting factors. This formulation presents significant computational challenges due to its multi-block structure, non-convexity, non-smoothness, and the absence of global gradient Lipschitz continuity. To address these challenges, we develop an accelerated alternating partial Bregman proximal gradient method (AAPB), whose distinctive feature lies in its capability to enable simultaneous updates of multiple variables. Under mild and theoretically justified assumptions, we establish both sublinear and global convergence properties of the proposed algorithm. Through careful selection of kernel generating distances tailored to various regularization terms, we derive corresponding closed-form solutions while maintaining the  $L$ -smooth adaptable property always holds for any  $L \geq 1$ . Numerical experiments, on graph regularized clustering and sparse NMF basis compression confirm the effectiveness of our model and algorithm.

**Keywords:** Low-rank, ReLU activation function, alternating minimization, Bregman method, acceleration.

## 1 Introduction

Exploring the low-rank structure inherent in real-world data is a fundamental technique within the applied mathematics and machine learning community [8]. Specifically, given a matrix  $M \in \mathbb{R}^{m \times n}$ , the low-rank approximation method assumes that  $M$  can be effectively approximated by a low-rank matrix, i.e.,

$$M \approx X, \quad X \text{ is low-rank.} \quad (1)$$

---

\*School of Mathematics and Computational Science, Xiangtan University, Xiangtan, 411105, China. Email: nothing2wang@hotmail.com

†LMIB, School of Mathematical Sciences, Beihang University, Beijing 100191, China. Email: yunfei.math@hotmail.com

‡LMIB, School of Mathematical Sciences, Beihang University, Beijing 100191, China. Email: chunfengcui@buaa.edu.cn

§Corresponding author. LMIB, School of Mathematical Sciences, Beihang University, Beijing 100191, China. Email: handr@buaa.edu.cn

Prominent low-rank decomposition methodologies encompass two fundamental approaches: the truncated singular value decomposition (TSVD) [17] and non-negative matrix factorization (NMF) [21, 27]. These established techniques have been widely adopted in various applications due to their theoretical foundations and practical effectiveness [53].

However, in practical applications, the observed data often deviates from the ideal low-rank assumption, thereby limiting the applicability of models based on the assumption in (1). This limitation becomes particularly pronounced when dealing with large-scale, non-negative, and sparse matrices [41, 42]. A notable example is the identity matrix, which, despite being highly sparse, inherently possesses full rank. Direct application of low-rank approximation to such data structures may consequently fail to capture and exploit their intrinsic structural properties. Given the fundamental importance and ubiquitous applications of sparse non-negative matrices in diverse scientific domains, investigating their inherent low-rank properties through activation functions has garnered significant research attention. These matrices play pivotal roles in numerous applications, including but not limited to: dimensionality reduction [15, 29], hyperspectral unmixing [24, 55], advanced signal processing [26, 31], and community detection in complex networks [28, 54]. This widespread applicability has motivated extensive research into understanding and exploiting their underlying low-rank structures through activation function-based approaches.

A deeper understanding of the intricate relationship between low-rankness and sparsity can be achieved by extending beyond conventional linear algebraic decomposition methods [47, 53]. In a significant contribution to this field, Saul [41] investigated the intrinsic low-rank characteristics of non-negative sparse matrices through an innovative approach. Specifically, the study focused on developing a nonlinear matrix decomposition (NMD) framework that, given a non-negative sparse matrix  $M \in \mathbb{R}^{m \times n}$ , seeks to identify a real-valued matrix  $X$  of equal or lower rank than  $M$  as follows,

$$M \approx \max(0, X), \quad X \text{ is low-rank}, \quad (2)$$

where  $\max(0, \cdot)$  is the rectified linear unit (ReLU) function, which is widely-used as the activation function for deep neural networks [23]. This indicates that when  $M$  is sparse, we are able to explore a large space where the zero entries may be any non-positive values and seek a low-rank matrix [42]. A particularly insightful example from [41] demonstrates the remarkable capability of this approach: for an  $n \times n$  identity matrix  $M$ , there exists a matrix  $X$  satisfying  $M = \max(0, X)$  with  $\text{rank}(X) \leq 3$  regardless of the dimension  $n$ . This striking result, maintaining rank-3 decomposition for identity matrices of arbitrary size, has propelled significant research interest in NMD, as evidenced by recent studies [32, 41, 48].

Mathematically, the ReLU-based NMD (ReLU-NMD) model approximates the expression in (2) by minimizing a least squares objective function, while predefinedly setting the rank of  $X$  to be a positive integer  $r$  that is less than  $\min(m, n)$ , i.e.,

$$\begin{aligned} \min_{X \in \mathbb{R}^{m \times n}} \quad & \frac{1}{2} \|M - \max(0, X)\|_F^2, \\ \text{s.t.} \quad & \text{rank}(X) = r. \end{aligned} \quad (3)$$

For notational simplicity, we denote the index set comprising zero and positive elements in  $M$  as

$$I_0 := \{(i, j) \mid M_{ij} = 0\} \quad (4)$$

and

$$I_+ := \{(i, j) \mid M_{ij} > 0\}, \quad (5)$$

respectively.

The objective function delineated in (3) is characterized by the absence of both differentiability and convexity. Furthermore, the intrinsic nonlinearity introduced by the ReLU function leads to

(3) has no closed-form solution and exacerbates the complexity of numerical methods. In light of these challenges, Saul [41] subsequently proposed an alternative formulation of ReLU-NMD, incorporating a slack variable  $W$ , defined as

$$\begin{aligned} \min_{X,W} \quad & \frac{1}{2} \|W - X\|_F^2, \\ \text{s.t.} \quad & \text{rank}(X) = r, \max(0, W) = M. \end{aligned} \quad (6)$$

The main advantage of this new formulation is that the low-rank constraints and the nonlinear activation function are separate, allowing for the exploration of new solution strategies. However, almost all algorithms for solving (6), such as [41, 42], require computing a rank- $r$  TSVD [17] at each iteration, which can be computationally expensive, especially for large matrices.

To circumvent this computationally expensive step, Seraghiti et al. [43] suggested replacing  $X \in \mathbb{R}^{m \times n}$  with the product  $UV$ , where  $U \in \mathbb{R}^{m \times r}$  and  $V \in \mathbb{R}^{r \times n}$ . Consequently, the problem (6) can be reformulated as

$$\begin{aligned} \min_{U,V,W} \quad & \frac{1}{2} \|W - UV\|_F^2, \\ \text{s.t.} \quad & \max(0, W) = M. \end{aligned} \quad (7)$$

A three-block nonlinear matrix decomposition algorithm (3B-NMD) was proposed in [43] to solve this optimization problem (7). The advantage of this algorithm is that each subproblem has a closed-form solution, and extrapolation techniques can be implemented to accelerate the convergence. Their experiments showed remarkable results compared with the baselines, but both  $U$ - and  $V$ -subproblems might experience numerical instability.

Recently, Wang et al. [49] explored a Tikhonov-regularized version of (7) represented as

$$\begin{aligned} \min_{U,V,W} \quad & \frac{1}{2} \|W - UV\|_F^2 + \frac{\eta}{2} \|U\|_F^2 + \frac{\eta}{2} \|V\|_F^2, \\ \text{s.t.} \quad & \max(0, W) = M, \end{aligned} \quad (8)$$

where  $\eta > 0$  is a predefined parameter. One advantage of model (8) is its ability to prevent overly aggressive steps in the alternating least-squares procedures in the 3B-NMD algorithm for the problem (7). However, all the above models fail to consider more comprehensive scenarios of the matrix factors  $U$  and  $V$ , such as low-rankness, sparsity or non-negativity. These structures are crucial for mitigating over-fitting, bolstering generalization capabilities, and enhancing solution stability.

To bridge these gaps, this paper proposes a more generalized and inclusive model as follows,

$$\begin{aligned} \min_{U,V,W} \quad & \frac{1}{2} \|W - UV\|_F^2 + H_1(U) + H_2(V), \\ \text{s.t.} \quad & \max(0, W) = M, \end{aligned} \quad (9)$$

where functions  $H_1(\cdot)$ ,  $H_2(\cdot)$  represent regularization terms, such as nuclear norm [39],  $l_2$  norm [22],  $l_1$  norm [46], or non-convex sparse terms [18, 56], which play the roles of regularizer promoting low-complexity structures such as low-rankness, sparsity or non-negativity of the solution.

The optimization problem (9) presents significant computational challenges due to its multi-block structure, non-convexity, non-smoothness, and the absence of global gradient Lipschitz continuity. One state-of-the-art approach to solving the multi-block problem is the alternating minimization method, which iteratively minimizes the objective function by fixing all variables except one. While leveraging the block structure can be intuitive and efficient, convergence is only assured when the minimum in each step is uniquely determined [3]. To ensure the uniqueness of

the minimum at each step, Attouch et al. [3] introduced the proximal alternating minimization (PAM) method. However, the subproblems in PAM typically lack closed-form solutions, limiting the algorithm’s practical performance. To address this limitation, Bolte et al. [9] developed an approximation method for PAM via proximal linearization, resulting in the proximal alternating linearized minimization (PALM) algorithm. Several inertial versions have been proposed to enhance the numerical performance of PALM, including iPALM [38], GiPALM [20], and NiPALM [50]. However, the convergence analysis of the alternating schemes usually requires the variable in the objective function to exhibit a global Lipschitz continuous gradient, which fails to hold for the matrix decomposition problems [10, 34].

To overcome these limitations and build the convergence in the absence of global Lipschitz continuous gradient, a generalization of the classical gradient Lipschitz continuity concept becomes essential. This generalization was initially proposed in [7] and subsequently developed for nonconvex optimization frameworks in [10]. The fundamental approach utilizes a generalized proximity measure based on Bregman distance, which serves as the foundation for the Bregman proximal gradient (BPG) method. This method extends the conventional proximal gradient approach by substituting Euclidean distances with Bregman distances as proximity measures. The corresponding convergence theory is established through a generalized Lipschitz condition, known as the  $L$ -smooth adaptable ( $L$ -smad) property [10]. Compared to PALM-type methods, the BPG-type algorithm offers several advantages [34]. First, BPG methods rely on a global  $L$ -smad constant, which is computed only once, simplifying the process. Second, block updates can be simultaneous, making BPG particularly effective for many matrix decomposition optimization problems [33]. Additionally, BPG-type methods are highly versatile, allowing for a broader range of applications. This flexibility opens up opportunities to design new loss functions and regularizers, without being limited to Lipschitz continuous gradients.

Despite the growth of BPG-type algorithms in recent literature, none have effectively exploited the specific structure of problem (9). Existing methods, including BPG [10], inertial BPG (iBPG) [35], DCAe [37], and BPDCA [45], are primarily designed for single-block optimization problems, although several of these methods have been extended to address two-block variable applications in their respective studies. In contrast, our problem (9) presents unique computational advantages when its multi-block structure is properly leveraged. Although some studies, such as BMME [25], have addressed multi-block optimization by applying BPG to individual subproblems, our approach is fundamentally distinguished by the  $W$ -subproblem in (9) admitting a closed-form solution - a distinctive feature that sets our method apart from existing frameworks. A comprehensive summary is presented in Table 1.

**Contribution.** In this paper, we establish a general model (9) to connect the non-negative sparsity and low-rank properties through the ReLU activation function. Additionally, we present a novel and efficient algorithm tailored to address this model. The key contributions are outlined as follows.

- (i) **Model:** We first propose a novel nonlinear matrix decomposition framework incorporating a comprehensive regularization term designed to simultaneously promote structures such as low-rankness, sparsity, and non-negativity in the resulting factors.
- (ii) **Algorithm:** Combining the ideas of alternating minimization and Bregman algorithms, we propose an alternating accelerated partial Bregman (AAPB) algorithm (Algorithm 1) for a general two-block nonconvex nonsmooth problem (12) which includes (9) as a special case. We then apply the AAPB algorithm to solve the optimization problem (9), see Algorithm 2 for details which denotes NMD-AAPB. Under the Kurdyka-Łojasiewicz (KL) property and some suitable conditions, the algorithm’s sublinear convergence rate and global convergence are also established.
- (iii) **Efficiency:** We present the closed-form solutions of the  $(U, V)$ - subproblem for several cases

Table 1: Summary of mentioned algorithms in Section 1. “-” indicates that the property is not analyzed in their paper, while “SCR” stands for subsequence convergence rate. “Single/Two” indicates that the theoretical analysis focuses on a single-variable case, but the method is applied to two-variable problems in their work; this interpretation similarly applies to “Multi/Two” and “Two/Multi”.

Algorithms	$L$ -smooth	Blocks	Extrapolation	SCR	Global under KL
PALM [9]	Yes	Multi	No	-	Yes
iPALM [38]	Yes	Multi	Yes	-	Yes
GiPALM [20]	Yes	Two	Yes	-	Yes
NiPALM [50]	Yes	Two	Yes	-	Yes
BPG [10]	No	Single	No	$\mathcal{O}(1/K)$	Yes
iBPG [35]	No	Single/Two	Yes	$\mathcal{O}(1/K)$	Yes
BPDCA(e) [45]	No	Single	Yes	$\mathcal{O}(1/K)$	Yes
DCAe [37]	No	Single/Two	Yes	-	Yes
BMME [25]	No	Multi/Two	Yes	-	Yes
This paper	No	Two/Multi	Yes	$\mathcal{O}(1/K)$	Yes

of  $H_1(U)$  and  $H_2(V)$ , which can be updated simultaneously while preserving the  $L$ -smooth adaptable property (Definition 9) for any  $L \geq 1$ . Numerical experiments on graph regularized clustering and sparse NMF basis compression demonstrate the effectiveness of the proposed model and algorithm.

The rest of this paper is organized as follows. Section 2 provides some relevant definitions and results which will be used in this paper. Section 3 provides an in-depth exposition of the proposed algorithm (Algorithm 1 and its special case Algorithm 2). We establish the sublinear convergence and global convergence results of the proposed algorithm and present the closed-form solution of the proposed algorithm under different regularizations in Sections 4 and 5, respectively. Section 6 utilizes synthetic and real datasets to demonstrate the stability of model (9) and the efficacy of the proposed algorithm, respectively. Finally, we draw conclusions in Section 7.

## 2 Preliminaries

In this section, we provide a concise summary of pivotal definitions and associated results that are important to the discussions in this paper.

**Definition 1.** [6] A function  $f : \mathbb{R}^d \rightarrow \mathbb{R}$  is  $\sigma$ -strongly convex if

$$f(y) \geq f(x) + \langle \nabla f(x), y - x \rangle + \frac{\sigma}{2} \|y - x\|^2$$

for any  $x, y \in \mathbb{R}^d$ .

**Definition 2.** [6] The proximal operator (also called the proximal mapping) associated with a (typically convex) function  $f : \mathbb{R}^d \rightarrow \mathbb{R}$ , is defined, for every  $x \in \mathbb{R}^d$  with  $\lambda > 0$ , as the following minimizer,

$$\text{prox}_{\lambda f}(x) := \arg \min_{y \in \mathbb{R}^d} f(y) + \frac{1}{2\lambda} \|y - x\|^2.$$

**Definition 3.** [16] For any  $x \in \mathbb{R}^d$ ,

$$S_\tau(x) = \arg \min_{y \in \mathbb{R}^d} \{ \tau \|y\|_1 + \frac{1}{2} \|y - x\|^2 \} = \max\{|y| - \tau, 0\} \text{sign}(y)$$

with the absolute value understood to be componentwise.

**Definition 4.** [30] Given  $x \in \mathbb{R}^d$ , without loss of generality we assume that  $|x_1| \geq |x_2| \geq \dots \geq |x_d|$ , then the hard-thresholding operator  $H_s(x)$  is given by

$$H_s(x) = \arg \min_{y \in \mathbb{R}^d} \{ \|y - x\|^2 : \|y\|_0 \leq s \} = \begin{cases} x_i, & \text{if } i \leq s, \\ 0, & \text{otherwise.} \end{cases}$$

**Definition 5.** [40] Let  $f : \mathbb{R}^d \rightarrow \mathbb{R} \cup \{+\infty\}$  be proper and lower semicontinuous. The basic limiting-subdifferential of  $f$  at  $x \in \text{dom } f$ , denoted by  $\partial f(x)$ , is defined by

$$\partial f(x) := \{g \in \mathbb{R}^d : \exists x_k \rightarrow x, f(x_k) \rightarrow f(x), g_k \in \hat{\partial} f(x_k) \text{ with } g_k \rightarrow g\}.$$

where  $\hat{\partial} f(\bar{x})$  denotes the Fréchet subdifferential of  $f$  at  $\bar{x} \in \text{dom } f$ , which is the set of all  $g \in \mathbb{R}^d$  satisfying

$$\liminf_{y \neq \bar{x}, y \rightarrow \bar{x}} \frac{f(y) - f(\bar{x}) - \langle g, y - \bar{x} \rangle}{\|y - \bar{x}\|} \geq 0.$$

**Definition 6.** ([3] Kurdyka-Lojasiewicz (KL) inequality): Let  $f : \mathbb{R}^d \rightarrow \mathbb{R} \cup \{+\infty\}$  be a proper lower semicontinuous function. For  $-\infty < \eta_1 < \eta_2 \leq +\infty$ , set

$$[\eta_1 < f < \eta_2] = \{x \in \mathbb{R}^d : \eta_1 < f(x) < \eta_2\}.$$

We say that function  $f$  has the KL property at  $x^* \in \text{dom } \partial f$  if there exist  $\eta \in (0, +\infty]$ , a neighborhood  $U$  of  $x^*$ , and a continuous concave function  $\phi : [0, \eta) \rightarrow \mathbb{R}_+$ , such that

- (1)  $\phi(0) = 0$ ;
- (2)  $\phi$  is  $C^1$  on  $(0, \eta)$  and continuous at 0;
- (3)  $\phi'(s) > 0, \forall s \in (0, \eta)$ ;
- (4)  $\forall x \in U \cap [f(x^*) < f < f(x^*) + \eta]$ , the following KL inequality holds

$$\phi'(f(x) - f(x^*))d(0, \partial f(x)) \geq 1,$$

where  $d(x, \Omega) = \inf_{y \in \Omega} \|x - y\|^2$  for any compact set  $\Omega$ .

**Definition 7.** ([4] KL function): We denote  $\Phi_\eta$  as the set of functions which satisfy (1)-(3) in Definition 6. If  $f$  satisfies the KL property at each point of  $\text{dom } \partial f$ , then  $f$  is called a KL function.

For a matrix  $X \in \mathbb{R}^{m \times n}$ , we denote its Frobenius norm by  $\|X\|_F := \sqrt{\sum_{i,j} x_{ij}^2}$ , the  $l_1$  norm  $\|X\|_1 := \sum_{i=1}^m \sum_{j=1}^n |x_{ij}|$ , the  $l_0$  norm  $\|X\|_0$  indicates the number of non-zero elements in matrix  $X$ . For a matrix  $Y \in \mathbb{R}^{m \times m}$ , we denote its trace as  $\text{Tr}(Y) := \sum_{i=1}^m Y_{ii}$ .

## 2.1 Bregman proximal gradient method

**Definition 8.** ([5, 10] Kernel-generating distance). Let  $C$  be a nonempty, convex, and open subset of  $\mathbb{R}^d$ . Associated with  $C$  and its closure  $\bar{C}$ , a function  $\psi : \mathbb{R}^d \rightarrow (-\infty, +\infty]$  is called a kernel generating distance if it satisfies the following conditions:

- (i)  $\psi$  is proper, lower semicontinuous, and convex, with  $\text{dom } \psi \subset \bar{C}$  and  $\text{dom } \partial\psi = C$ .
- (ii)  $\psi$  is  $C^1$  on  $\text{int } \text{dom } \psi \equiv C$ .

The class of kernel-generating distances is denoted by  $\mathcal{G}(C)$ . Given  $\psi \in \mathcal{G}(C)$ , we can define the proximity measure  $D_\psi : \text{dom } \psi \times \text{int } \text{dom } \psi \rightarrow \mathbb{R}_+$  by

$$D_\psi(x, y) := \psi(x) - \psi(y) - \langle \nabla\psi(y), x - y \rangle. \quad (10)$$

The proximity measures  $D_\psi$  is also called the Bregman distance [12]. It measures the proximity of  $x$  and  $y$ .

Indeed,  $\psi$  is convex if and only if  $D_\psi(x, y) \geq 0$  for any  $x \in \text{dom } \psi$  and  $y \in \text{int } \text{dom } \psi$ .

We examine the following optimization problem to introduce the Bregman proximal gradient (BPG) method,

$$\min_{x \in \bar{C}} f(x) + h(x),$$

where  $f$  is a continuously differentiable (possibly nonconvex) function that may not have a globally Lipschitz continuous gradient,  $h$  is an extended-valued function (possibly nonconvex),  $C$  is a nonempty, convex, open subset in  $\mathbb{R}^d$ .

The BPG mapping defined in [10] is formulated as follows

$$\begin{aligned} x^{k+1} &\in \underset{x \in \bar{C}}{\text{argmin}} \left\{ h(x) + \langle \nabla f(x^k), x - x^k \rangle + \frac{1}{\lambda} D_\psi(x, x^k) \right\} \\ &= \underset{x \in \mathbb{R}^d}{\text{argmin}} \left\{ h(x) + \langle \nabla f(x^k), x - x^k \rangle + \frac{1}{\lambda} D_\psi(x, x^k) \right\}, \end{aligned}$$

where  $\lambda > 0$  is the step size. When  $\psi = \frac{1}{2} \|\cdot\|^2$ , this method simplifies to the classic proximal gradient descent algorithm [6].

The key to the convergence analysis is the  $L$ -smooth adaptable property shown as follows.

**Definition 9.** ([10]  $L$ -smooth adaptable ( $L$ -smad)) Given  $\psi \in \mathcal{G}(C)$ , let  $f : \mathcal{X} \rightarrow (-\infty, +\infty]$  be a proper and lower semi-continuous function with  $\text{dom } \psi \subset \text{dom } f$ , which is continuously differentiable on  $C$ . We say  $(f, \psi)$  is  $L$ -smad on  $C$  if there exists  $L > 0$  such that for any  $x, y \in C$ ,

$$|f(x) - f(y) - \langle \nabla f(y), x - y \rangle| \leq LD_\psi(x, y). \quad (11)$$

If  $\psi(\cdot) = \frac{1}{2} \|\cdot\|^2$ , then it reduces to the  $L$ -smooth [36].

## 3 Algorithm

In this section, we present an efficient algorithm to solve the optimization problem (9). Firstly, we consider a more general two-block optimization framework that naturally encompasses the model (9) as a specific instance, i.e.,

$$\min_{Y \in C_1, W \in C_2} \Phi(Y, W) := F(Y, W) + G(W) + H(Y), \quad (12)$$

where  $C_1, C_2$  are closed convex sets,  $F(Y, W)$  is a smooth but nonconvex function, and  $G(W)$  and  $H(Y)$  are two nonsmooth (possibly nonconvex) functions. In particular, this non-convex non-smooth optimization problem exhibits the following two key characteristics: Firstly, the  $W$ -subproblem has a closed-form solution; Secondly, the  $Y$ -subproblem does not have a closed-form solution, and  $\nabla_Y F(Y, W)$  is not global Lipschitz continuous for any fixed  $W$ . Building on these two points, and considering the limitations of the existing BPG-type algorithms as discussed earlier, it is essential to design a new, efficient solution algorithm tailored to the specific characteristics of the proposed model.

By leveraging the strengths of alternating minimization [9, 51], we first propose the alternating partial Bregman (APB) method, as shown below,

$$\begin{cases} W^{k+1} \in \operatorname{argmin}_{W \in C_2} F(Y^k, W) + G(W), \\ Y^{k+1} \in \operatorname{argmin}_{Y \in C_1} H(Y) + \langle \nabla_Y F(Y^k, W^{k+1}), Y - Y^k \rangle + \frac{1}{\lambda} D_\psi(Y, Y^k). \end{cases}$$

Here, we utilize the closed-form solution in the  $W$ -subproblem and apply the BPG [10, 33] in the  $Y$ -subproblem, specifically to tackle the issue that  $\nabla_Y F(Y, W)$  is not global Lipschitz continuous. Here,  $D_\psi(\cdot, \cdot)$  is the Bregman distance defined by Definition 8.

However, the numerical performance of this framework may not be optimal. To accelerate the convergence and get better numerical performance, we incorporate the extrapolation technique [35] to the variable  $Y$ , i.e.,

$$\bar{Y}^k = Y^k + \beta_k(Y^k - Y^{k-1}).$$

and

$$Y^{k+1} \in \operatorname{argmin}_{Y \in C_1} H(Y) + \langle \nabla_Y F(\bar{Y}^k, W^{k+1}), Y - \bar{Y}^k \rangle + \frac{1}{\lambda} D_\psi(Y, \bar{Y}^k). \quad (13)$$

It is the extrapolation step to accelerate the convergence and  $\beta_k \in [0, 1)$ . Then the accelerated version of the APB (AAPB) algorithm is established, see Algorithm 1 for details. When  $\beta_k = 0$ , then the AAPB algorithm reduces to the APB algorithm.

---

**Algorithm 1 AAPB:** Accelerated alternating Partial Bregman algorithm for the optimization problem (12).

---

**Input:**  $0 < \lambda \leq 1/L$ ,  $K$ , and kernel-generating distance  $\psi$ .

**Initialization:**  $Y^0 = Y^{-1}$ ,

1: **for**  $k = 0, 1, \dots, K$  **do**

2:   Update  $W^{k+1} \in \operatorname{argmin}_{W \in C_2} F(Y^k, W) + G(W)$ .

3:   Compute  $\bar{Y}^k = Y^k + \beta_k(Y^k - Y^{k-1}) \in C_1$  with  $\beta_k \in [0, 1)$ .

4:   Update

$$Y^{k+1} \in \operatorname{argmin}_{Y \in C_1} H(Y) + \langle \nabla_Y F(\bar{Y}^k, W^{k+1}), Y - \bar{Y}^k \rangle + \frac{1}{\lambda} D_\psi(Y, \bar{Y}^k).$$

5: **end for**

**Output:**  $Y^{k+1}$ .

---

### 3.1 AAPB algorithm for (9)

In this subsection, we apply the AAPB algorithm (Algorithm 1) to solve the optimization problem (9). For a comprehensive understanding, please refer to Algorithm 2 for details.



---

**Algorithm 2 NMD-AAPB:** The AAPB algorithm for the optimization problem (9)

---

**Input:**  $M, r, 0 < \lambda \leq 1/L, I_+, I_0, K$ , and kernel-generating distance  $\psi$ .

**Initialization:**  $U^0 = U^{-1}, V^0 = V^{-1}, X^0 = U^0 V^0$ , and set  $W_{i,j} = M_{i,j}$  for  $(i, j) \in I_+$ .

- 1: **for**  $k = 0, 1, \dots, K$  **do**
- 2:   Compute  $W_{i,j}^{k+1} = \min(0, X_{i,j}^k)$  for  $(i, j) \in I_0$ .
- 3:   Compute  $\bar{U}^k = U^k + \beta_k(U^k - U^{k-1})$  and  $\bar{V}^k = V^k + \beta_k(V^k - V^{k-1})$ , where  $\beta_k \in [0, 1]$ .
- 4:   Update

$$\begin{aligned} P^k &:= \lambda \nabla_U F(\bar{U}^k, \bar{V}^k, W^{k+1}) - \nabla_U \psi(\bar{U}^k, \bar{V}^k), \\ Q^k &:= \lambda \nabla_V F(\bar{U}^k, \bar{V}^k, W^{k+1}) - \nabla_V \psi(\bar{U}^k, \bar{V}^k). \end{aligned}$$

$$\begin{aligned} (U^{k+1}, V^{k+1}) \in \operatorname{argmin} \{ &\lambda H_1(U) + \lambda H_2(V) \\ &+ \langle P^k, U \rangle + \langle Q^k, V \rangle + \psi(U, V) \}. \end{aligned} \quad (14)$$

- 5:   Compute  $X^{k+1} = U^{k+1} V^{k+1}$ .

6: **end for**

**Output:**  $U^{k+1}, V^{k+1}$ .

---

Now we give the details of the proposed algorithm (Algorithm 2) designed to solve the optimization problem (9) as follows.

**W-subproblem:** At the  $k$ -th iteration,

$$W^{k+1} = \operatorname{argmin}_{\max(0, W) = M} \frac{1}{2} \|W - X^k\|_F^2,$$

where  $X^k = U^k V^k$ . Then we derive the closed-form solution  $W^{k+1}$  as

$$W_{i,j}^{k+1} = \begin{cases} M_{i,j}, & \text{if } (i, j) \in I_+, \\ \min(0, X_{i,j}^k), & \text{if } (i, j) \in I_0. \end{cases}$$

Here,  $I_0$  and  $I_+$  are defined by (4) and (5), respectively.

**(U, V)-subproblem** For the general formulation of  $H_1(U)$  and  $H_2(V)$ , the subproblem

$$(U^{k+1}, V^{k+1}) \in \operatorname{argmin}_{U, V} F(U, V, W^{k+1}) + H_1(U) + H_2(V)$$

may not have a closed-form solution in general. Inspired by the works in [10, 34], we propose the application of the Bregman proximal gradient method to the  $(U, V)$ -subproblem. Denote  $F_k := F(\bar{U}^k, \bar{V}^k, W^{k+1})$ , thus we have

$$\begin{aligned} (U^{k+1}, V^{k+1}) \in &\operatorname{argmin}_{U, V} H_1(U) + H_2(V) + \langle \nabla_U F_k, U - \bar{U}^k \rangle \\ &+ \langle \nabla_V F_k, V - \bar{V}^k \rangle + \frac{1}{\lambda} D_\psi((U, V), (\bar{U}^k, \bar{V}^k)) \\ = &\operatorname{argmin}_{U, V} H_1(U) + H_2(V) + \langle \nabla_U F_k, U - \bar{U}^k \rangle \\ &+ \langle \nabla_V F_k, V - \bar{V}^k \rangle + \frac{1}{\lambda} (\psi(U, V) - \psi(\bar{U}^k, \bar{V}^k)) \\ &- \langle \nabla_U \psi(\bar{U}^k, \bar{V}^k), U - \bar{U}^k \rangle - \langle \nabla_V \psi(\bar{U}^k, \bar{V}^k), V - \bar{V}^k \rangle \end{aligned}$$

$$=\operatorname{argmin}_{U,V} \lambda H_1(U) + \lambda H_2(V) + \langle P^k, U \rangle + \langle Q^k, V \rangle + \psi(U, V),$$

where  $\lambda$  is the step size, and

$$\begin{aligned} P^k &:= \lambda \nabla_U F(\bar{U}^k, \bar{V}^k, W^{k+1}) - \nabla_U \psi(\bar{U}^k, \bar{V}^k), \\ Q^k &:= \lambda \nabla_V F(\bar{U}^k, \bar{V}^k, W^{k+1}) - \nabla_V \psi(\bar{U}^k, \bar{V}^k). \end{aligned}$$

**Remark 1.** Algorithm 2 presents two distinct advantages:

- (i) As stated in Proposition 1 in Subsection 5, for the  $(U, V)$ -subproblem, any  $L \geq 1$  satisfies the  $L$ -smad property. This eliminates the practical necessity for estimation.
- (ii) The  $(U, V)$ -subproblem can be updated simultaneously in the proposed algorithm, which significantly reduces computational time in numerical experiments. This advantage is particularly notable when dealing with large-scale data.

## 4 Convergence analysis

In this section, we present the sublinear convergence and global convergence results of the AAPB algorithm (Algorithm 1) for solving (12) as follows. Prior to presenting these results, we outline the necessary assumptions. It is important to note that, within the context of this paper  $C = \mathbb{R}^n$  in Definition 8.

**Assumption 1.** Assume the following conditions hold:

- (i) The kernel generating distance  $\psi$  given by Definition 8, is  $\sigma$ -strongly convex.
- (ii)  $F$  is a continuously differentiable function and the functions pair  $(F(\cdot, W), \psi)$  is  $L$ -smooth adaptable (see Definition 9).
- (iii)  $G, H$  are two proper, lower semicontinuous functions.
- (iv)  $\Phi^* := \inf_{Y, W} \Phi(Y, W) > -\infty$ .
- (v) There exists  $\alpha \in \mathbb{R}$  such that  $H(\cdot) - \frac{\alpha}{2} \|\cdot\|_F^2$  is convex.

If  $\beta_k = 0$  in Algorithm 1, Assumption 1 (v) can be removed, and the convergence results also hold.

**Assumption 2.** We assume the parameter  $\beta_k \in [0, 1)$  in Algorithm 1 satisfies the following inequality,

$$D_\psi(Y^k, \bar{Y}^k) \leq \frac{\delta - \varepsilon}{1 + L\lambda} D_\psi(Y^{k-1}, Y^k),$$

where  $1 > \delta > \varepsilon > 0$ ,  $\lambda$  denotes the step size in the proposed algorithms, while  $L$  is the parameter defined in Definition 9.

A remark regarding Assumption 2 is provided as follows.

**Remark 2.** When  $\psi = \frac{1}{2} \|\cdot\|_F^2$ , it follows from Assumption 2 that

$$\beta_k \leq \sqrt{\frac{\delta - \varepsilon}{1 + L\lambda}}.$$

In other words, if  $\delta - \varepsilon \approx 1$ , one could choose the extrapolation parameter  $\beta_k \approx 1/\sqrt{2}$ . In general, the closed-form expression for  $\beta_k$  is difficult to obtain in each iteration. One possible approach is to apply the backtracking line-search strategy [35] to find a proper  $\beta_k$  such that the inequality in Assumption 2 holds. However, this technique may be time-consuming. For simplicity, we set this parameter as a fixed constant.

We further demonstrate the convergence of the proposed algorithm under the KL property, as presented in the following two theorems.

**Theorem 1.** *(Subsequence convergence of Algorithm 1) Assume Assumptions 1 and 2 hold, and  $0 < \lambda \leq 1/L$ . Let  $\{Y^k\}_{k \in \mathbb{N}}$  be the sequence generated by the NMD-AAPB algorithm. Then the following statements hold.*

(i) We have

$$\sum_{k=1}^{+\infty} D_\psi(Y^{k-1}, Y^k) < +\infty,$$

which indicates the sequence  $D_\psi(Y^{k-1}, Y^k)$  converges to zero with  $k \rightarrow +\infty$ .

(ii) In addition, we have

$$\min_{1 \leq k \leq K} D_\psi(Y^{k-1}, Y^k) = \mathcal{O}(1/K).$$

*Proof.* From the  $W$ -subproblem in Algorithm 1, we obtain

$$F(Y^k, W^{k+1}) + G(W^{k+1}) \leq F(Y^k, W^k) + G(W^k). \quad (15)$$

Given the convexity of  $H(Y) - \frac{\alpha}{2}\|Y\|_F^2$  as stated in Assumption 1, we can derive that

$$H(Y^k) - \frac{\alpha}{2}\|Y^k\|_F^2 \geq H(Y^{k+1}) - \frac{\alpha}{2}\|Y^{k+1}\|_F^2 + \langle \xi^{k+1} - \alpha Y^{k+1}, Y^k - Y^{k+1} \rangle,$$

where  $\xi^{k+1} \in \partial H(Y^{k+1})$ . It can be reformulated equivalently as follows,

$$H(Y^{k+1}) + \frac{\alpha}{2}\|Y^{k+1} - Y^k\|_F^2 + \langle \xi^{k+1}, Y^k - Y^{k+1} \rangle \leq H(Y^k).$$

From the first-order optimality condition of the  $Y$ -subproblem in Algorithm 1, we can derive that

$$\xi^{k+1} + \nabla_Y F(\bar{Y}^k, W^{k+1}) + \frac{1}{\lambda}(\nabla \psi(Y^{k+1}) - \nabla \psi(\bar{Y}^k)) = 0.$$

By combining the above two inequalities, we can derive the following result

$$\begin{aligned} & H(Y^{k+1}) + \frac{\alpha}{2}\|Y^{k+1} - Y^k\|_F^2 - \langle \nabla_Y F(\bar{Y}^k, W^{k+1}), Y^k - Y^{k+1} \rangle \\ & + \frac{1}{\lambda} \langle \nabla \psi(\bar{Y}^k) - \nabla \psi(Y^{k+1}), Y^k - Y^{k+1} \rangle \\ = & H(Y^{k+1}) + \frac{\alpha}{2}\|Y^{k+1} - Y^k\|_F^2 - \langle \nabla_Y F(\bar{Y}^k, W^{k+1}), Y^k - Y^{k+1} \rangle \\ & + \frac{1}{\lambda} (D_\psi(Y^k, Y^{k+1}) + D_\psi(Y^{k+1}, \bar{Y}^k) - D_\psi(Y^k, \bar{Y}^k)) \\ \leq & H(Y^k), \end{aligned} \quad (16)$$

where the last equality follows from the three-point identity. Furthermore, since  $F(\cdot, W)$  is an  $L$ -smad function with respect to  $\psi$ , we have

$$\begin{aligned} & F(Y^{k+1}, W^{k+1}) - F(\bar{Y}^k, W^{k+1}) \\ \leq & \langle \nabla_Y F(\bar{Y}^k, W^{k+1}), Y^{k+1} - \bar{Y}^k \rangle + LD_\psi(Y^{k+1}, \bar{Y}^k), \end{aligned}$$

and

$$F(\bar{Y}^k, W^{k+1}) + \langle \nabla_Y F(\bar{Y}^k, W^{k+1}), Y^k - \bar{Y}^k \rangle$$

$$\leq F(Y^k, W^{k+1}) + LD_\psi(Y^k, \bar{Y}^k).$$

By combining the above two inequalities, we have

$$\begin{aligned} F(Y^{k+1}, W^{k+1}) &\leq F(Y^k, W^{k+1}) + \langle \nabla_Y F(\bar{Y}^k, W^{k+1}), Y^{k+1} - Y^k \rangle \\ &\quad + LD_\psi(Y^k, \bar{Y}^k) + LD_\psi(Y^{k+1}, \bar{Y}^k). \end{aligned} \quad (17)$$

By summing inequalities (15), (16) and (17) together, we obtain

$$\begin{aligned} &\Phi(Y^{k+1}, W^{k+1}) \\ &\leq \Phi(Y^k, W^k) + (L + \frac{1}{\lambda})D_\psi(Y^k, \bar{Y}^k) - \frac{1}{\lambda}D_\psi(Y^k, Y^{k+1}) \\ &\quad + (L - \frac{1}{\lambda})D_\psi(Y^{k+1}, \bar{Y}^k) - \frac{\alpha}{2}\|Y^{k+1} - Y^k\|_F^2 \\ &\leq \Phi(Y^k, W^k) + (L + \frac{1}{\lambda})D_\psi(Y^k, \bar{Y}^k) - \frac{1}{\lambda}D_\psi(Y^k, Y^{k+1}) - \frac{\alpha}{2}\|Y^{k+1} - Y^k\|_F^2, \end{aligned}$$

where the last inequality follows from  $\lambda L \leq 1$ . We define, with  $k \in \mathbb{N}$ , the following Lyapunov sequence

$$\Theta^k := \lambda(\Phi(Y^k, W^k) - \Phi^*) + \delta D_\psi(Y^{k-1}, Y^k).$$

Then we can derive that

$$\begin{aligned} &\Theta^k - \Theta^{k+1} \\ &= \lambda\Phi(Y^k, W^k) + \delta D_\psi(Y^{k-1}, Y^k) - \lambda\Phi(Y^{k+1}, W^{k+1}) - \delta D_\psi(Y^k, Y^{k+1}) \\ &\geq \delta D_\psi(Y^{k-1}, Y^k) + (1 - \delta)D_\psi(Y^k, Y^{k+1}) + \frac{\alpha\lambda}{2}\|Y^{k+1} - Y^k\|_F^2 \\ &\quad - (1 + L\lambda)D_\psi(Y^k, \bar{Y}^k) \\ &\geq (\frac{\alpha\lambda}{2} + \frac{(1 - \delta)\sigma}{2})\|Y^{k+1} - Y^k\|_F^2 + \delta D_\psi(Y^{k-1}, Y^k) - (1 + L\lambda)D_\psi(Y^k, \bar{Y}^k) \\ &\geq \delta D_\psi(Y^{k-1}, Y^k) - (\delta - \epsilon)D_\psi(Y^{k-1}, Y^k) \\ &= \epsilon D_\psi(Y^{k-1}, Y^k), \end{aligned}$$

where the second inequality follows from  $1 - \delta > 0$ , the  $\sigma$ -strong convexity of  $\psi$  and  $\lambda^{-1} \geq L \geq -\alpha(1 - \delta)\sigma$ , and the third inequality follows from Assumption 2. Then we have

$$\sum_{k=1}^K D_\psi(Y^{k-1}, Y^k) \leq \frac{1}{\epsilon}(\Theta^1 - \Theta^{K+1}) \leq \frac{1}{\epsilon}\Theta^1.$$

Taking  $K \rightarrow +\infty$ , we obtain that

$$\sum_{k=1}^{+\infty} D_\psi(Y^{k-1}, Y^k) < +\infty,$$

from which we immediately deduce that the sequence  $\{D_\psi(Y^{k-1}, Y^k)\}$  converges to zero.

In addition, we also have

$$K \min_{1 \leq k \leq K} D_\psi(Y^{k-1}, Y^k) \leq \sum_{k=1}^K D_\psi(Y^{k-1}, Y^k) \leq \frac{1}{\epsilon}\Theta^1,$$

which yields the desired result. This completes the proof.  $\square$

The above theorem could only establish the sub-sequential convergence of the AAPB algorithm if the sequence remains in a bounded set. We also require the following assumption to analyze the global convergence. It should be emphasized that the local Lipschitz continuity assumption for both  $\nabla F(Y, W)$  and  $\nabla \psi$  is sufficient in this paper, which is a weaker requirement compared to global Lipschitz continuity.

**Assumption 3.** *We assume the following two conditions hold:*

- (i)  $\nabla F(Y, W)$  is Lipschitz continuous with constant  $L_1 > 0$  on any bounded subset of  $\text{dom}F$ .
- (ii)  $\nabla \psi$  is Lipschitz continuous with constant  $L_2 > 0$  on any bounded subset of  $\text{dom}\psi$ .

Based on the above theorem, combined with the KL framework [9], we demonstrate the whole sequence convergence as follows.

**Theorem 2.** *(Global convergence of Algorithm 1) Suppose that Assumptions 1, 2 and 3 hold, and  $0 < \eta \leq 1/L$ . Let  $\{Z^k := (Y^k, W^k)\}_{k \in \mathbb{N}}$  be a bounded sequence generated by the AAPB algorithm. Assume that the optimization function  $\Phi(Y, W)$  is a semi-algebraic function [4] that satisfies the KL property with exponent  $\theta \in [0, 1)$  (see Definition 7). Then either the point  $Z^k$  is a critical point after a finite number of iterations or the sequence  $\{Z^k\}_{k \in \mathbb{N}}$  satisfies the finite length property,*

$$\sum_{k=0}^{+\infty} \|Z^{k+1} - Z^k\|_F < +\infty.$$

*Proof.* From the optimality condition of  $Y$ - and  $W$ -subproblems in Algorithm 1, we have

$$\begin{cases} 0 \in \partial H(Y^{k+1}) + \nabla_Y F(\bar{Y}^k, W^{k+1}) + \frac{1}{\lambda}(\nabla \psi(Y^{k+1}) - \nabla \psi(\bar{Y}^k)), \\ 0 \in \nabla_W F(Y^k, W^{k+1}) + \partial G(W^{k+1}). \end{cases} \quad (18)$$

Denote

$$\begin{aligned} A_1^{k+1} &:= \nabla_Y F(Y^{k+1}, W^{k+1}) - \nabla_Y F(\bar{Y}^k, W^{k+1}) - \frac{1}{\lambda}(\nabla \psi(Y^{k+1}) - \nabla \psi(\bar{Y}^k)), \\ A_2^{k+1} &:= \nabla_W F(Y^{k+1}, W^{k+1}) - \nabla_W F(Y^k, W^{k+1}). \end{aligned}$$

We have

$$A_1^{k+1} \in \nabla_Y F(Y^{k+1}, W^{k+1}) + \partial H(Y^{k+1}), \quad A_2^{k+1} \in \nabla_W F(Y^{k+1}, W^{k+1}) + \partial G(W^{k+1}).$$

Consequently,  $A^{k+1} = (A_1^{k+1}, A_2^{k+1}) \in \partial \Phi(Y^{k+1}, W^{k+1})$  and

$$\begin{aligned} & \|A^{k+1}\|_F \\ & \leq \|A_1^{k+1}\|_F + \|A_2^{k+1}\|_F \\ & = \|\nabla_Y F(Y^{k+1}, W^{k+1}) - \nabla_Y F(\bar{Y}^k, W^{k+1}) - \frac{1}{\lambda}(\nabla \psi(Y^{k+1}) - \nabla \psi(\bar{Y}^k))\|_F \\ & \quad + \|\nabla_W F(Y^{k+1}, W^{k+1}) - \nabla_W F(Y^k, W^{k+1})\|_F \\ & \leq \|\nabla_Y F(Y^{k+1}, W^{k+1}) - \nabla_Y F(\bar{Y}^k, W^{k+1})\|_F + \frac{1}{\lambda} \|\nabla \psi(Y^{k+1}) - \nabla \psi(\bar{Y}^k)\|_F \\ & \quad + \|\nabla_W F(Y^{k+1}, W^{k+1}) - \nabla_W F(Y^k, W^{k+1})\|_F \\ & \leq (L_1 + \frac{L_2}{\lambda}) \|Y^{k+1} - \bar{Y}^k\|_F + L_1 \|Y^{k+1} - Y^k\|_F \\ & \leq (2L_1 + \frac{L_2}{\lambda}) \|Y^{k+1} - Y^k\|_F + \beta_k (L_1 + \frac{L_2}{\lambda}) \|Y^k - Y^{k-1}\|_F, \end{aligned}$$

where the third inequality follows from Assumption 3, and the last inequality follows from  $\bar{Y}^k = Y^k + \beta_k(Y^k - Y^{k-1})$  and triangle inequality.

Furthermore, under the assumption that the function  $\Phi(Y, W)$  is a proper, lower semi-continuous, and semi-algebraic function [4], it satisfies the KL property at every point within its domain  $\text{dom}\Phi$ . By incorporating Definition 7 and Theorem 1, we can deduce that the sequence  $\{Z^k\}$  generated is indeed a Cauchy sequence. The comprehensive proof of this theorem bears resemblance to Theorem 4.5 in [2] and Theorem 4.2 in [25]. Thus the details are omitted for brevity.  $\square$

It is worth noting that if the fixed step size  $\lambda$  in the proposed algorithm (Algorithm 1) is changed to an adaptive case  $\lambda_k$ , the convergence results of the proposed algorithm still hold if  $\lambda_k \leq \min\{\lambda_{k-1}, 1/L\}$ .

## 5 Closed-form solutions

In this section, we provide a detailed analysis of the closed-form solutions for the  $(U, V)$ -subproblem under different cases of  $H_1(U)$  and  $H_2(V)$ .

First, we present the  $L$ -smad property for the term  $F(U, V, W^{k+1}) = \frac{1}{2}\|W^{k+1} - UV\|_F^2$  in the content of matrix decomposition. The following two propositions (Propositions 1 and 2) are similar to the corresponding results in [33, 34, 52] with some straightforward modifications. The primary difference between our kernel generating distance and those in [33, 34, 52] is that theirs is fixed, whereas ours changes with the number of iterations due to the fact that BPG is incorporated in our AAPB framework. However, the basic proof process remains largely unchanged, so we omit the proof here for simplicity. Interested readers can refer to the details in [33, 34, 52].

**Proposition 1.** *At the  $k$ -th iteration, let  $F(U, V, W^{k+1}) = \frac{1}{2}\|W^{k+1} - UV\|_F^2$ ,  $\psi_1 = \left(\frac{\|U\|_F^2 + \|V\|_F^2}{2}\right)^2$ ,  $\psi_2 = \frac{\|U\|_F^2 + \|V\|_F^2}{2}$ . Then, for any  $L \geq 1$ , the function  $F$  satisfies the  $L$ -smad property (Definition 9) with respect to the following kernel generating distance*

$$\psi(U, V) = 3\psi_1(U, V) + \|W^{k+1}\|_F \psi_2(U, V). \quad (19)$$

Now, we discuss the closed-form solution for  $(U, V)$  in the NMD-AAPB algorithm (i.e., (14) in Algorithm 2) for several cases of  $H_1(U)$  and  $H_2(V)$ . The Bregman distances for  $(U, V)$ -subproblem under different cases of  $H_1(U) + H_2(V)$  are given in Table 2. Then the corresponding closed-form solutions are given in the following proposition.

Table 2: The Bregman distances for  $(U, V)$ -subproblem under different cases of  $H_1(U) + H_2(V)$  at the  $k$ -th iteration.

Case	$H_1(U) + H_2(V)$	$\psi(U, V)$
(i)	$0 + 0$	$3\psi_1(U, V) + \ W^{k+1}\ _F \psi_2(U, V)$
(ii)	$\frac{\eta_1}{2}\ U\ _F^2 + \frac{\eta_2}{2}\ V\ _F^2$	$3\psi_1(U, V) + \ W^{k+1}\ _F \psi_2(U, V)$
(iii)	$\eta_1\ U\ _1 + \eta_2\ V\ _1$	$3\psi_1(U, V) + \ W^{k+1}\ _F \psi_2(U, V)$
(iv)	$\frac{\mu_0}{2}\text{Tr}(U^T LU) + \frac{\eta_1}{2}\ U\ _F^2 + \frac{\eta_2}{2}\ V\ _F^2$	$3\psi_1(U, V) + (\ W^{k+1}\ _F + \mu_0\ L\ _F)\psi_2(U, V)$
(v)	$\eta_1\ U\ _1 - \frac{\eta_2}{2}\ U\ _F^2$	$3\psi_1(U, V) + \ W^{k+1}\ _F \psi_2(U, V) + \frac{\eta_2\lambda}{2}\ U\ _F^2$
(vi)	$I_{\ U, \cdot\ _0 \leq s_1} + I_{\ V, \cdot\ _0 \leq s_2}$	$3\psi_1(U, V) + \ W^{k+1}\ _F \psi_2(U, V)$

**Proposition 2.** *In this proposition, we provide the closed-form solutions of  $(U, V)$ -subproblem as follows.*

(i)  $\mathbf{H}_1(\mathbf{U}) = \mathbf{H}_2(\mathbf{V}) = \mathbf{0}$ . At the  $k$ -th iteration, the closed-form solutions of  $(U^{k+1}, V^{k+1})$  are given by  $U^{k+1} = -tP^k$ ,  $V^{k+1} = -tQ^k$  respectively, where  $t$  is the non-negative real root of

$$3(\|P^k\|_F^2 + \|Q^k\|_F^2)t^3 + \|W^{k+1}\|_F t - 1 = 0.$$

(ii)  $\mathbf{H}_1(\mathbf{U}) = \frac{\eta_1}{2}\|\mathbf{U}\|_F^2$ ,  $\mathbf{H}_2(\mathbf{V}) = \frac{\eta_2}{2}\|\mathbf{V}\|_F^2$ . At the  $k$ -th iteration, the closed-form solutions  $(U^{k+1}, V^{k+1})$  are given by  $U^{k+1} = -t_1P^k$ ,  $V^{k+1} = -t_2Q^k$  respectively, where  $t_1$  and  $t_2$  are the non-negative real root of

$$3(\|P^k\|_F^2 + \|Q^k\|_F^2)t^3 + (\|W^{k+1}\|_F + \eta_1)t - 1 = 0$$

and

$$3(\|P^k\|_F^2 + \|Q^k\|_F^2)t^3 + (\|W^{k+1}\|_F + \eta_2)t - 1 = 0,$$

respectively.

(iii)  $\mathbf{H}_1(\mathbf{U}) = \eta_1\|\mathbf{U}\|_1$ ,  $\mathbf{H}_2(\mathbf{V}) = \eta_2\|\mathbf{V}\|_1$ . At the  $k$ -th iteration, the update step (14) is given by  $U^{k+1} = t\mathcal{S}_{\eta_1\lambda}(-P^k)$ ,  $V^{k+1} = t\mathcal{S}_{\eta_2\lambda}(-Q^k)$  respectively, where  $t \geq 0$  and satisfies

$$3(\|\mathcal{S}_{\eta_1\lambda}(-P^k)\|_F^2 + \|\mathcal{S}_{\eta_2\lambda}(-Q^k)\|_F^2)t^3 + \|W^{k+1}\|_F t - 1 = 0,$$

where  $\mathcal{S}_\lambda(\cdot)$  is the soft-thresholding operator, see Definition 3 for details.

(iv)  $\mathbf{H}_1(\cdot) = \frac{\mu_0}{2}\text{Tr}(\mathbf{U}^T\mathbf{L}\mathbf{U}) + \frac{\eta_1}{2}\|\mathbf{U}\|_F^2$ ,  $\mathbf{H}_2(\cdot) = \frac{\eta_2}{2}\|\mathbf{V}\|_F^2$ . At the  $k$ -th iteration, the update step of  $(U, V)$  is given by  $U^{k+1} = -t_1P^k$ ,  $V^{k+1} = -t_2Q^k$  respectively, where  $t_1, t_2 \geq 0$  and satisfies

$$3(\|P^k\|_F^2 + \|Q^k\|_F^2)t^3 + (\|W^{k+1}\|_F + \mu_0\|L\|_F + \eta_1)t - 1 = 0$$

and

$$3(\|P^k\|_F^2 + \|Q^k\|_F^2)t^3 + (\|W^{k+1}\|_F + \mu_0\|L\|_F + \eta_2)t - 1 = 0,$$

respectively.

(v)  $\mathbf{H}_1(\mathbf{U}) = \eta_1\|\mathbf{U}\|_1 - \frac{\eta_2}{2}\|\mathbf{U}\|_F^2$ ,  $\mathbf{H}_2(\mathbf{V}) = \mathbf{0}$ . At the  $k$ -th iteration, the update step (14) is given by  $U^{k+1} = t\mathcal{S}_{\eta_1\lambda}(-P^k)$ ,  $V^{k+1} = -tQ^k$  respectively, where  $t \geq 0$  and satisfies

$$3(\|\mathcal{S}_{\eta_1\lambda}(-P^k)\|_F^2 + \| - Q^k \|_F^2)t^3 + \|W^{k+1}\|_F t - 1 = 0.$$

(vi)  $\mathbf{H}_1(\mathbf{U}) = \mathbf{I}_{\|\mathbf{U}\|_0 \leq s_1}$ ,  $\mathbf{H}_2(\mathbf{V}) = \mathbf{I}_{\|\mathbf{V}\|_0 \leq s_2}$ . At the  $k$ -th iteration, the update step (14) is given by  $U^{k+1} = t\mathcal{H}_{s_1}(-P^k)$ ,  $V^{k+1} = t\mathcal{H}_{s_2}(-Q^k)$  respectively, where  $t \geq 0$  and satisfies

$$3(\|\mathcal{H}_{s_1}(-Q^k)\|_F^2 + \|\mathcal{H}_{s_2}(-Q^k)\|_F^2)t^3 + \|W^{k+1}\|_F t - 1 = 0,$$

where  $\mathcal{H}_s(\cdot)$  is the hard-thresholding operator, see Definition 4 for details.

**Remark 3.** The  $t$ -subproblem in the above proposition requires solving a one-dimensional cubic equation as follows,

$$at^3 + ct - 1 = 0,$$

where  $a, c > 0$ . The unique positive solution [19] would be  $t = \frac{-\sqrt[3]{\alpha_1} - \sqrt[3]{\alpha_2}}{3a}$  with  $\alpha_1 = 3a(\frac{-9a + \sqrt{81a^2 + 12ac^3}}{2})$  and  $\alpha_2 = 3a(\frac{-9a - \sqrt{81a^2 + 12ac^3}}{2})$ , respectively.

## 6 Numerical experiments

This section presents numerical experiments evaluating the real-world performance of our proposed algorithm under varying regularization strengths. Experiments are implemented in MATLAB using a system equipped with a 3.4 GHz Intel Core i7-14700KF processor and 64 GB RAM.

The algorithm terminates if one of the following three conditions is met:

- (a) The maximum run time ( $\max_T$ ) is reached.
- (b) The maximum number of iterations ( $\max_K$ ) is reached.
- (c) All algorithms for ReLU-based models of the synthetic dataset terminate when

$$\text{Tol} := \frac{\|M - \max(0, UV)\|_F}{\|M\|_F} \leq 10^{-4}.$$

All algorithms for ReLU-based models of the real dataset will use the following quantity

$$\text{Tol} := \frac{\|M - \max(0, X)\|_F}{\|M\|_F} \leq e_{\min},$$

where  $X$  is the solution, and  $e_{\min}$  is the smallest relative error obtained by all algorithms within the allotted time.

For simplicity, we set the extrapolation parameter<sup>1</sup>  $\beta_k = 0.6$  for the NMD-AAPB algorithm, and set the step size  $\lambda \leq 1/L$  with  $L \geq 1$  from Proposition 1 for all the proposed algorithms. This section presents the analysis of the regularization methods associated with cases (iii), (iv), and (vi) in Table 2, with each case being investigated separately.

### 6.1 Graph regularized matrix factorization

Extensive research in the literature [1, 14, 44] has demonstrated the effectiveness of matrix decomposition techniques for clustering problems, particularly in document and image clustering applications. However, a critical limitation of these existing approaches lies in their reliance on strict nonnegativity constraints  $U, V \geq 0$ , which may excessively restrict the solution space compared to the more flexible constraint  $UV \geq 0$ . This stringent requirement often leads to suboptimal low-rank approximations. To address this limitation, we propose to relax the non-negative constraints and consider the following optimization problem:

$$\begin{aligned} \min_{U, V, W} \quad & \frac{1}{2} \|W - UV\|_F^2 + \frac{\mu_0}{2} \text{Tr}(U^T \bar{L} U) + \frac{\eta_1}{2} \|U\|_F^2 + \frac{\eta_2}{2} \|V\|_F^2, \\ \text{s.t.} \quad & \max(0, W) = M. \end{aligned} \tag{20}$$

where  $\text{Tr}(U^T \bar{L} U)$  is the graph-regularization term,  $\text{Tr}(\cdot)$  denotes the trace of a matrix,  $\bar{L}$  denotes the graph Laplacian matrix, and  $\mu_0$ ,  $\eta_1$  and  $\eta_2$  are three positive parameters. We use three datasets<sup>2</sup> *COIL20*, *PIE*, and *TDT2* (see Table 3 for details) to illustrate the numerical performance of the proposed algorithm. In this numerical experiment, we let  $\mu_0 = 100$ , and  $r = 20$  for *COIL20*,  $r = 68$  for *PIE*,  $r = 100$  for *COIL100*, and  $r = 30$  for *TDT2*, respectively.

<sup>1</sup>Here,  $\beta_k = 0.6$  is taken simply to meet the conditions in Remark 2. A larger value or an adaptive approach can be employed, as numerical experiments demonstrate that convergence is still guaranteed and potentially improved numerical results can be obtained.

<sup>2</sup><http://www.cad.zju.edu.cn/home/dengcai/Data/data.html>



Table 3: The details for three datasets. “sparsity (%)” stands for the proportion of non-zero elements in the data.

Data	$m$	$n$	$r$	sparsity (%)
<i>PIE</i>	2856	1024	68	91.47
<i>COIL20</i>	1440	1024	20	65.61
<i>TDT2</i>	9394	36771	30	0.35

We compute the clustering labels by applying the  $K$ -means method<sup>3</sup> to the matrix  $U$ . The clustering accuracy, defined as the proportion of correctly predicted class labels between the obtained labels and the ground truth labels, is computed following the methodology described in [13]. Additionally, we conduct a comprehensive comparison between our proposed ReLU-based graph matrix decomposition model (20) and the well-established graph-regularized NMF framework [14]. Specifically,

$$\min_{U \in \mathbb{R}_+^{m \times r}, V \in \mathbb{R}_+^{r \times n}} \frac{1}{2} \|M - UV\|_F^2 + \frac{\mu_0}{2} \text{Tr}(U^T L U) + \frac{\eta_1}{2} \|U\|_F^2 + \frac{\eta_2}{2} \|V\|_F^2. \quad (21)$$

We employ two advanced optimization approaches: the BPG method [10] and its enhanced variant, BPG with extrapolation (BPGE) [35, 52] to address this optimization problem.

For both clustering models, we set the parameters as follows:  $\mu_0 = 100$ ,  $\eta_1 = \eta_2 = 0.1$ . To maintain consistency across all datasets, we implemented a uniform stopping criterion of  $\max_k = 100$  for all algorithms. The clustering performance was evaluated using accuracy metrics, with detailed methodological references available in [13]. The comparative results of all algorithms across three datasets are systematically presented in Table 4. This table provides a clear overview of each algorithm’s performance in the clustering tasks.

Table 4: Comparison of clustering accuracy (%) on three datasets for models (20) and (21) under compared algorithms.

Data	K-means	model (21)		model (20)	
		BPG	BPGE	NMD-APB	NMD-AAPB
<i>PIE</i>	54.41	84.09	88.78	84.92	<b>88.80</b>
<i>COIL20</i>	73.86	86.74	87.62	87.60	<b>89.04</b>
<i>TDT2</i>	67.43	75.43	81.78	77.69	<b>84.24</b>

As evidenced by the results presented in Table 4, both the proposed ReLU-based model (20) and the classical graph-regularized NMF approach (21) significantly outperform the direct application of the K-means algorithm to the raw data matrix  $M$ . Furthermore, our proposed ReLU-based model (20) demonstrates superior clustering performance over the classical graph-regularized NMF approach (21). This empirical validation not only confirms the effectiveness of our proposed model but also highlights the computational efficiency of the accompanying algorithm. Notably, the accelerated version of our algorithm consistently outperforms its non-accelerated counterpart across all experimental scenarios.

A particularly interesting observation from Table 4 reveals a strong correlation between data sparsity and performance improvement: the sparser the dataset, the more significant the performance gains achieved by our ReLU-based decomposition model compared to traditional approaches.

<sup>3</sup><http://www.cad.zju.edu.cn/home/dengcai/Data/Clustering.html>

This trend suggests that the ReLU function’s inherent properties are particularly well-suited for handling sparse data structures.

Based on these comprehensive numerical results, we conclude that for applications involving non-negative sparse datasets, the ReLU-based optimization model represents a promising alternative that can potentially deliver enhanced numerical performance. This finding opens new possibilities for applying our approach to various real-world scenarios where sparse data representations are prevalent.

## 6.2 Compression of sparse NMF Basis

We now investigate an additional application of ReLU-NMD: the compression of sparse non-negative dictionaries [27]. To demonstrate this application, we employ two standard facial image datasets<sup>4</sup>: the *ORL* dataset with  $m = 4096$  features and  $n = 400$  samples, and the *YaleB* dataset with  $m = 1024$  features and  $n = 2414$  samples. Through the NMF decomposition framework  $M \approx \tilde{U}\tilde{V}$ , where both factor matrices  $\tilde{U}$  and  $\tilde{V}$  maintain non-negativity constraints, we can effectively extract sparse facial features that are represented by the columns of the basis matrix  $\tilde{U}$ .

Specifically, we implement a rank-100 NMF decomposition<sup>5</sup> on the *ORL* dataset, producing a sparse non-negative matrix  $\tilde{U} \in \mathbb{R}^{4096 \times 100}$ . Similarly, for the *YaleB* dataset, we perform a rank-81 NMF decomposition, resulting in  $\tilde{U} \in \mathbb{R}^{1024 \times 81}$ . Based on these decompositions, we further compress  $\tilde{U} \in \mathbb{R}^{m \times r}$  into a thin basis matrix  $U \in \mathbb{R}^{m \times r'}$ , where  $r' < r$  by the following optimization model:

$$\begin{aligned} \min_{U, V, W} \quad & \frac{1}{2} \|W - UV\|_F^2 + \sum_{i=1}^r J_{\|(V^T)_i\|_0 \leq s_2}, \\ \text{s.t.} \quad & \max(0, W) = \tilde{U}. \end{aligned} \quad (22)$$

Here,  $U \in \mathbb{R}^{m \times r'}$ ,  $V \in \mathbb{R}^{r' \times r}$ , and  $V_i$  is the  $i$ -th column of  $V$ . For simplicity, we set  $s_2 = \lfloor r/1.2 \rfloor$  to demonstrate the numerical performance of model (22) for the proposed algorithms. The performance of the compressed NMF is evaluated through the NMD relative error and the NMF relative error metric, defined as:

$$\text{Tol}_{\text{NMF}} := \min_{\hat{V} \geq 0} \frac{\|M - \max(0, UV)\hat{V}\|_F}{\|M\|_F}, \quad (23)$$

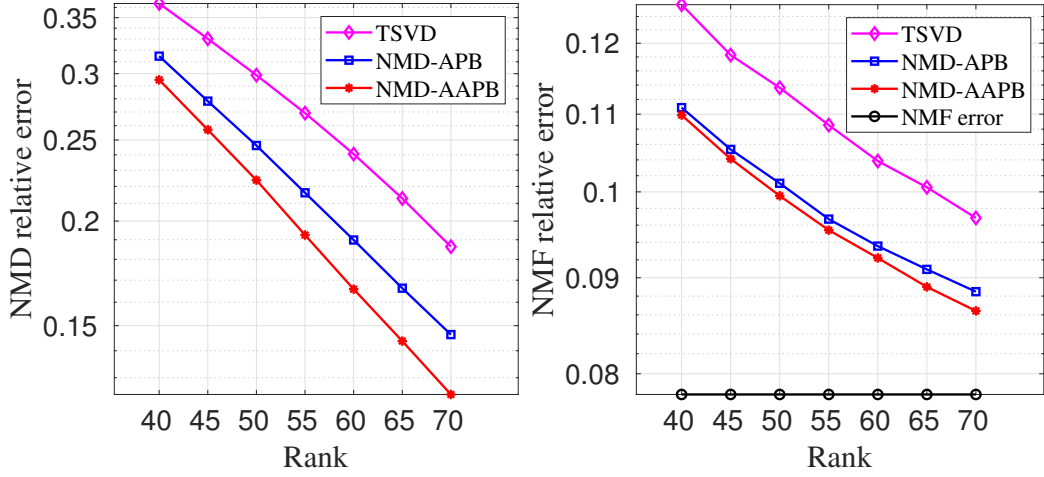
The results are visually presented in Figure 1, where Figure 1 (a) displays the compression of a 4096-by-100 NMF basis  $U$  from the *ORL* dataset, and Figure 1 (b) shows the compression of a 1024-by-81 NMF basis  $U$  from the *YaleB* dataset.

The numerical results presented in Figure 1 clearly illustrate that the proposed NMD-APB and NMD-AAPB outperform the baseline methods. This superiority can be attributed to the fact that the ReLU-based model is more adept at capturing the underlying structure of the dataset, and furthermore, the availability of a closed-form solution for the  $(U, V)$ -subproblem facilitates faster convergence.

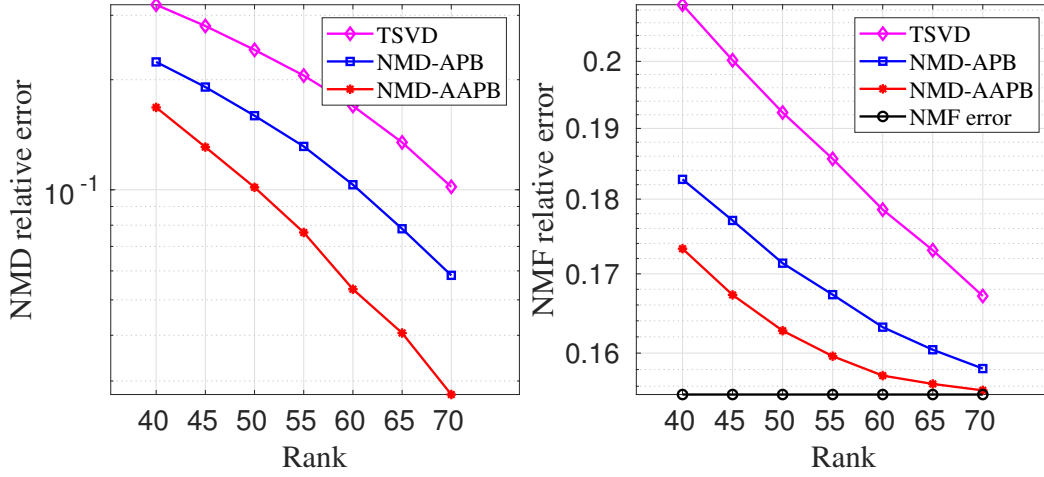
Additionally, Figure 2 presents an instance of a rank  $r = 55$  reconstruction derived from the original rank  $r = 81$  NMF factor for the *YaleB* dataset. We also show the details of the 80-th basis of  $U$  in Figure 3. This example further confirms the superior accuracy of the proposed model and algorithms in approximating the dataset.

<sup>4</sup><http://www.cad.zju.edu.cn/home/dengcai/Data/FaceData.html>

<sup>5</sup><https://gitlab.com/ngillis/nmfbook/>



(a) *ORL*. Left: Error on  $U$ . Right: Error on  $M$ .



(b) *YaleB*. Left: Error on  $U$ . Right: Error on  $M$ .

Figure 1: Numerical experiments of real-world datasets for solving (22).

### 6.3 $H_1(U) = \eta_1 \|U\|_1, H_2(V) = \eta_2 \|V\|_1$

In this subsection, we focus on the scenario where  $H_1(U) = \eta_1 \|U\|_1, H_2(V) = \eta_2 \|V\|_1$  in (9), which reformulated (9) equivalently as the following optimization problem

$$\begin{aligned} \min_{U, V, W} \quad & \frac{1}{2} \|W - UV\|_F^2 + \eta_1 \|U\|_1 + \eta_2 \|V\|_1, \\ \text{s.t.} \quad & \max(0, W) = M. \end{aligned} \quad (24)$$

For the above optimization problem, algorithms such as A-NMD, 3B-NMD, and NMD-TM are not suitable because both the  $U$ - and  $V$ -subproblems lack closed-form solutions. We compare our proposed methods with a PALM-type algorithm [9] that incorporates a partial linearization technique [51]. This variant is denoted as PPALM, given that the  $W$ -subproblem consistently admits a closed-form solution. Additionally, we take into account its inertial counterpart, referred

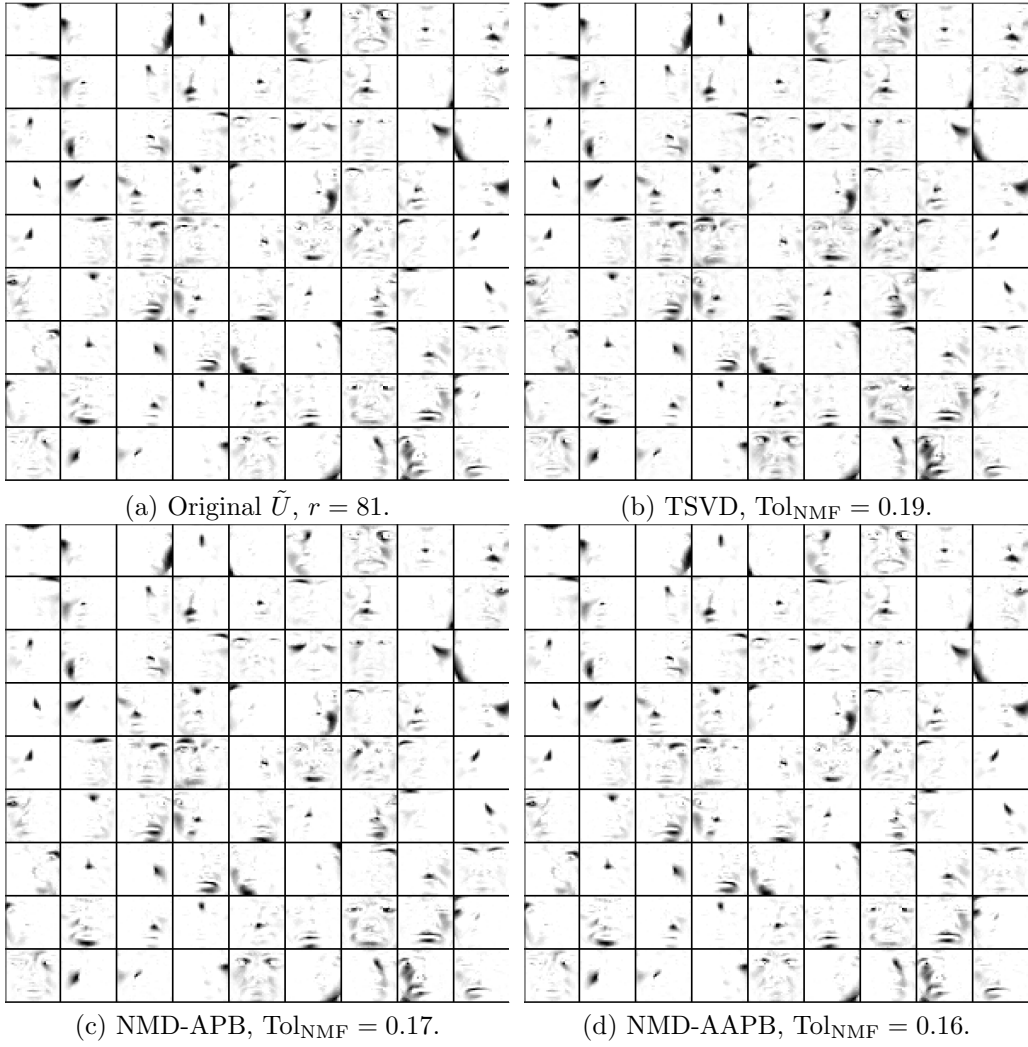


Figure 2: Original factor  $\tilde{U}$  of NMF for *YaleB* dataset, with rank- $r = 81$  and low-rank reconstruction by TSVD [11], NMD-APB and NMD-AAPB with fixed rank- $r = 55$ .



Figure 3: The 80-th basis of the factor  $U$  in Figure 2. Left to right: Original, TSVD [11], NMD-APB, NMD-AAPB.

to as iPPALM, which is a special case of iPAMPL [51]. For a comprehensive understanding, please refer to Algorithm 3 in Appendix A for further details.

We first consider the synthetic datasets generated by

$$M = \max(0, UV),$$

where  $U \in \mathbb{R}^{m \times r^*}$  and  $V \in \mathbb{R}^{r^* \times n}$  are generated by command “ $U = \text{randn}(m, r^*), U(\text{abs}(U) < 1) = 0$ ” and “ $V = \text{randn}(r^*, n), V(\text{abs}(V) < 1) = 0$ ” in MATLAB. We set  $\eta_1 = 0.01$ ,  $\eta_2 = 0.015$ ,  $\max_T = 20s$ , and  $\max_K = 1000$ .

The numerical experiments presented in Figure 4 demonstrate that NMD-APB and NMD-AAPB algorithms proposed in this paper converge faster than PPALM and iPPALM. One possible reason that NMD-APB and NMD-AAPB adopt the closed-form solution of the  $(U, V)$ -subproblem, while PPALM and iPPALM update the  $U$ - and  $V$ -subproblems by the proximal gradient descent approach separately. The acceleration technique yields superior numerical results compared to the vanilla versions. Additionally, a higher estimated rank corresponds to a better fit to the original data.

Next, we evaluate our approach on three real-world datasets: *netz4504-dual*, *mycielskian11*<sup>6</sup>, and the widely-used *MNIST* dataset<sup>7</sup>. The detailed characteristics and statistical properties of these datasets are presented in Table 5.

Table 5: The details for three real-world datasets applied in solving (24).

Data	$m$	$n$	sparsity (%)
<i>netz4504-dual</i>	615	615	0.62
<i>mycielskian11</i>	1535	1535	5.72
<i>MNIST</i>	$1000 \times 10$	784	19.27

We set  $\max_T = 30s$  and  $\max_K = 1000$  and show the numerical results in Table 6. It is evident from this table that, compared with PPALM and iPPALM, the algorithm proposed in this paper achieves better numerical results. Furthermore, NMD-AAPB converges faster than NMD-APB. The numerical performance is also confirmed in Figure 5.

Table 6: The relative error for three real-world datasets for solving optimization problem (24).

Data	rank ( $r$ )	PPALM	iPPALM	NMD-APB	NMD-AAPB
<i>netz4504-dual</i>	10	9.0e-1	6.2e-1	1.8e-1	<b>1.5e-1</b>
	15	7.2e-1	1.7e-1	4.9e-2	<b>6.2e-3</b>
	20	4.4e-1	2.4e-2	2.1e-2	<b>5.8e-4</b>
<i>mycielskian11</i>	15	6.0e-1	2.4e-1	1.3e-1	<b>9.3e-2</b>
	25	3.0e-1	1.3e-1	8.3e-2	<b>6.7e-2</b>
	35	2.1e-1	9.1e-2	6.2e-1	<b>4.1e-2</b>
<i>MNIST</i>	25	4.1e-1	3.5e-1	3.3e-1	<b>3.0e-1</b>
	35	3.8e-1	3.0e-1	2.7e-1	<b>1.7e-1</b>
$m = 1000 \times 10$	45	3.3e-1	2.8e-1	2.4e-1	<b>1.1e-1</b>

<sup>6</sup>Source: <https://sparse.tamu.edu/>

<sup>7</sup>Source: <http://yann.lecun.com/exdb/mnist/>

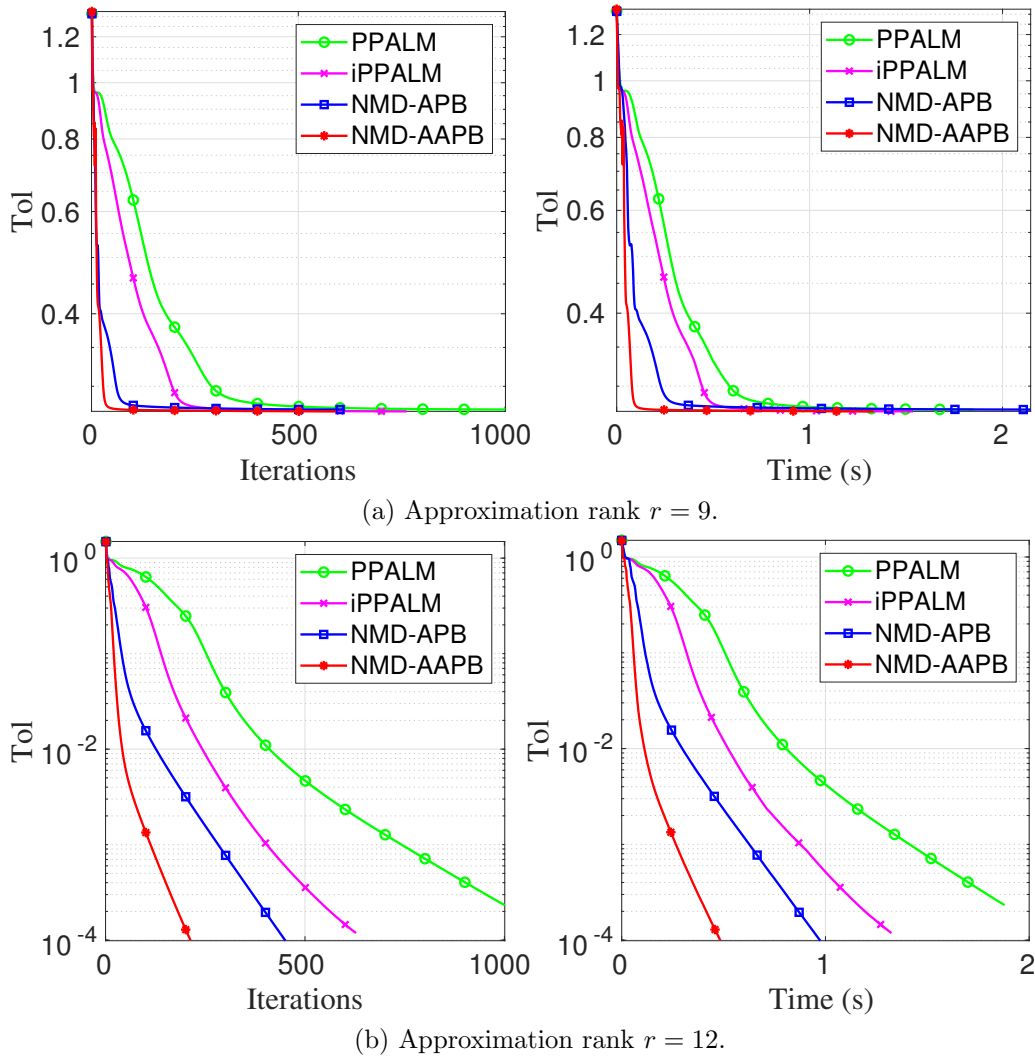


Figure 4: Numerical results for solving (24) with  $m = 1500, n = 500, r^* = 10$  by synthetic datasets.

## 7 Conclusion

In this paper, we investigated feature extraction and pattern recognition in sparse nonnegative matrices. While the original data may not inherently exhibit low-rank properties, we explored the intrinsic low-rank characteristics through the application of the ReLU activation function. We introduced a novel nonlinear matrix decomposition framework that incorporates comprehensive regularization terms, capable of addressing critical tasks such as graph-regularized clustering and sparse NMF basis compression. Specifically, we developed an accelerated alternating partial Bregman (AAPB) algorithm tailored for solving this model. From a theoretical perspective, we established both the sublinear and global convergence properties of the proposed algorithm. Extensive numerical experiments on graph-regularized clustering and sparse NMF basis compression tasks demonstrated the effectiveness and efficiency of our proposed model and algorithm.

The proposed model shows distinctive advantages in the following conditions: high sparsity in the dataset and the absence of closed-form solutions for the subproblems related to factor matrices.

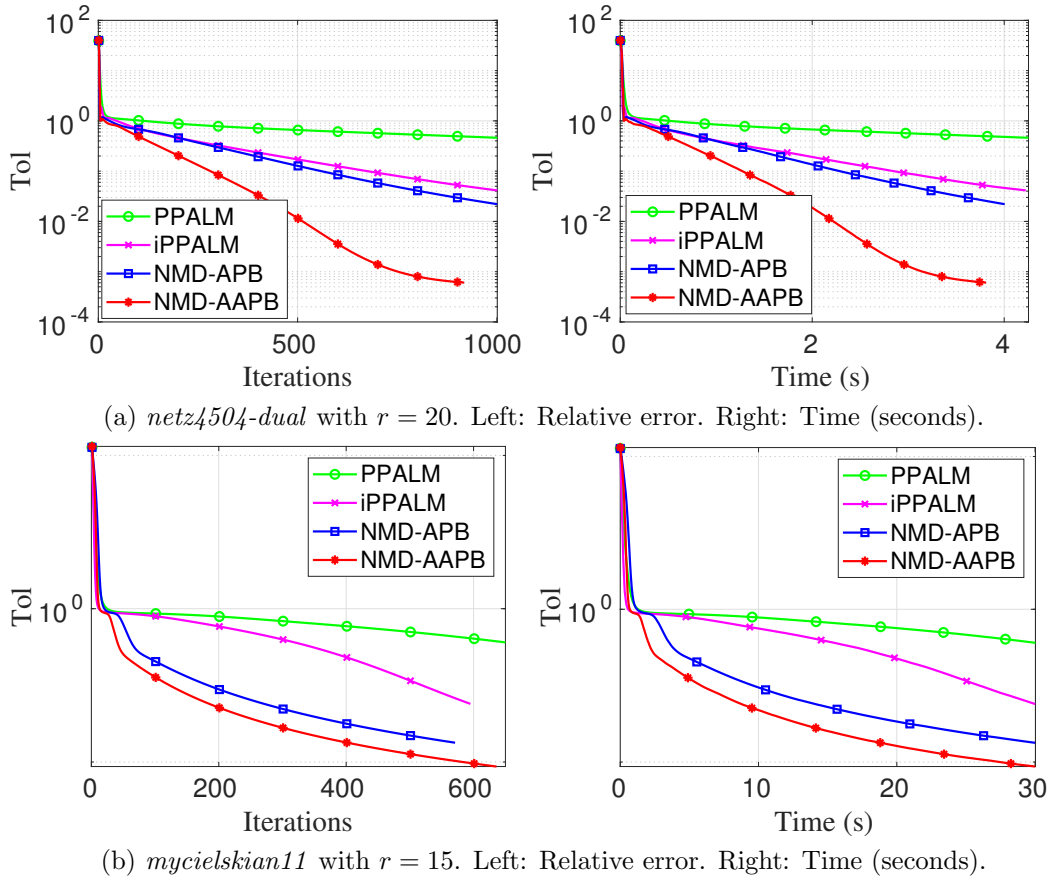


Figure 5: Numerical results for solving (24) by two real-world datasets.

In cases where closed-form solutions are attainable, i.e., the regularization terms in (9) are zeros or Tikhonov regularizations, the alternative algorithms such as 3B-NMD and NMD-TM may exhibit superior performance.

## A iPPALM framework

We present the framework of the inertial partial proximal alternating linearization minimization (iPPALM) algorithm for the optimization problem (9) (Algorithm 3). Note that when  $\beta_k = 0$  in Algorithm 3, it reduces to the partial proximal alternating linearization minimization (PPALM) method. Using the convergence analysis framework from [38, 51], we can also establish the global convergence result for the iPPALM algorithm.

## Declarations

**Funding:** This research is supported by the National Key R&D Program of China (No. 2021YFA1003600), the National Natural Science Foundation of China (NSFC) grants 12131004, 12401415, 12471282, the R&D project of Pazhou Lab (Huangpu) (Grant no. 2023K0603, 2023K0604), the Natural Science Foundation of Hunan Province (No. 2025JJ60009), and the Fundamental Research Funds for

---

**Algorithm 3 iPPALM:** Inertial partial proximal alternating linearization minimization for the optimization problem (9)

---

**Input:**  $M, r, I_+, I_0$ , and  $K$ . Bregman distance  $\psi$ .

**Initialization:**  $U^0, V^0, X^0 = U^0 V^0$ , and set  $W_{i,j} = M_{i,j}$  for  $(i, j) \in I_+$ .

1: **for**  $k = 0, 1, \dots, K$  **do**

2:   Compute  $W_{i,j}^{k+1} = \min(0, X_{i,j}^k)$  for  $(i, j) \in I_0$ .

3:   Compute  $\bar{U}^k = U^k + \beta_k(U^k - U^{k-1})$  with  $\beta_k \in [0, 1)$ , let  $\lambda_1^k > 0$  and update

$$U^{k+1} \in \underset{U}{\operatorname{argmin}} \langle \nabla_U F(\bar{U}^k, V^k, W^{k+1}), U - \bar{U}^k \rangle + \frac{1}{2\lambda_1^k} \|U - \bar{U}^k\|_F^2 + H_1(U).$$

4:   Compute  $\bar{V}^k = V^k + \beta_k(V^k - V^{k-1})$ , let  $\lambda_2^k > 0$  and update

$$V^{k+1} \in \underset{V}{\operatorname{argmin}} \langle \nabla_V F(U^{k+1}, \bar{V}^k, W^{k+1}), V - \bar{V}^k \rangle + \frac{1}{2\lambda_2^k} \|V - \bar{V}^k\|_F^2 + H_2(V).$$

5:   Compute  $X^{k+1} = U^{k+1} V^{k+1}$ .

6: **end for**

**Output:**  $X^{k+1}$ .

---

the Central Universities (Grant No. YWF-22-T-204).

**Competing interests:** The authors have no competing interests to declare that are relevant to the content of this article.

## References

- [1] I. Ahmed, X. B. Hu, M. P. Acharya, and Y. Ding. Neighborhood structure assisted non-negative matrix factorization and its application in unsupervised point-wise anomaly detection. *J. Mach. Learn. Res.*, 22:34:1–34:32, 2021.
- [2] M. Ahookhosh, L. T. K. Hien, N. Gillis, and P. Patrinos. Multi-block bregman proximal alternating linearized minimization and its application to orthogonal nonnegative matrix factorization. *Comput. Optim. Appl.*, 79(3):681–715, 2021.
- [3] H. Attouch, J. Bolte, P. Redont, and A. Soubeyran. Proximal alternating minimization and projection methods for nonconvex problems: An approach based on the Kurdyka-Lojasiewicz inequality. *Math. Oper. Res.*, 35(2):438–457, 2010.
- [4] H. Attouch, J. Bolte, and B. F. Svaiter. Convergence of descent methods for semi-algebraic and tame problems: proximal algorithms, forward-backward splitting, and regularized gauss-seidel methods. *Math. Program.*, 137(1-2):91–129, 2013.
- [5] A. Auslender and M. Teboulle. Interior gradient and proximal methods for convex and conic optimization. *SIAM J. Optim.*, 16(3):697–725, 2006.
- [6] A. Beck. *First-Order Methods in Optimization*. SIAM, 2017.



- [7] B. E. Birnbaum, N. R. Devanur, and L. Xiao. Distributed algorithms via gradient descent for fisher markets. In Y. Shoham, Y. Chen, and T. Roughgarden, editors, *Proceedings 12th ACM Conference on Electronic Commerce*, pages 127–136. ACM, 2011.
- [8] C. Bishop. *Pattern Recognition and Machine Learning*. Springer, 2006.
- [9] J. Bolte, S. Sabach, and M. Teboulle. Proximal alternating linearized minimization for non-convex and nonsmooth problems. *Math. Program.*, 146(1-2):459–494, 2014.
- [10] J. Bolte, S. Sabach, M. Teboulle, and Y. Vaisbourd. First order methods beyond convexity and Lipschitz gradient continuity with applications to quadratic inverse problems. *SIAM J. Optim.*, 28(3):2131–2151, 2018.
- [11] C. Boutsidis and M. Magdon-Ismail. Faster svd-truncated regularized least-squares. In *2014 IEEE International Symposium on Information Theory*, pages 1321–1325. IEEE, 2014.
- [12] L. Bregman. The relaxation method of finding the common point of convex sets and its application to the solution of problems in convex programming. *USSR Comput. Math. Math. Phys.*, 7(3):200–217, 1967.
- [13] D. Cai, X. He, and J. Han. Document clustering using locality preserving indexing. *IEEE Trans. Knowl. Data. Eng.*, 17(12):1624–1637, 2005.
- [14] D. Cai, X. He, J. Han, and T. S. Huang. Graph regularized non-negative matrix factorization for data representation. *IEEE Trans. Pattern. Anal. Mach. Intell.*, 33(8):1548–1560, 2011.
- [15] H. Che, J. Wang, and A. Cichocki. Bicriteria sparse nonnegative matrix factorization via two-timescale duplex neurodynamic optimization. *IEEE Trans. Neural Networks Learn. Syst.*, 34(8):4881–4891, 2023.
- [16] D. L. Donoho. De-noising by soft-thresholding. *IEEE Trans. Inf. Theory.*, 41(3):613–627, 1995.
- [17] C. Eckart and G. Young. The approximation of one matrix by another of lower rank. *Psychometrika*, 1(3):211–218, 1936.
- [18] J. Fan and R. Li. Variable selection via nonconcave penalized likelihood and its oracle properties. *J. Am. Stat. Assoc.*, 96(456):1348–1360, 2001.
- [19] S. Fan. A new extracting formula and a new distinguishing means on the one variable cubic equation. *Natur. Sci. J. Hainan Teachers College*, 2:91–98, 1989.
- [20] X. Gao, X. Cai, and D. Han. A Gauss-Seidel type inertial proximal alternating linearized minimization for a class of nonconvex optimization problems. *J. Glob. Optim.*, 76(4):863–887, 2020.
- [21] N. Gillis. *Nonnegative Matrix Factorization*. SIAM, Philadelphia, 2020.
- [22] G. H. Golub, P. C. Hansen, and D. P. O’Leary. Tikhonov regularization and total least squares. *SIAM J. Matrix Anal. Appl.*, 21(1):185–194, 1999.
- [23] I. Goodfellow, Y. Bengio, and A. Courville. *Deep Learning*. MIT Press, 2016.
- [24] Z. Guo, A. Min, B. Yang, J. Chen, H. Li, and J. Gao. A sparse oblique-manifold nonnegative matrix factorization for hyperspectral unmixing. *IEEE Trans. Geosci. Remote. Sens.*, 60:1–13, 2022.

- [25] L. T. K. Hien, D. N. Phan, N. Gillis, M. Ahoosh, and P. Patrinos. Block bregman majorization minimization with extrapolation. *SIAM J. Math. Data Sci.*, 4(1):1–25, 2022.
- [26] P. Humbert, B. L. Bars, L. Oudre, A. Kalogeratos, and N. Vayatis. Learning laplacian matrix from graph signals with sparse spectral representation. *J. Mach. Learn. Res.*, 22:195:1–195:47, 2021.
- [27] D. D. Lee and H. S. Seung. Learning the parts of objects by non-negative matrix factorization. *Nature*, 401(6755):788–791, 1999.
- [28] X. Li, Z. Hu, and H. Wang. Combining non-negative matrix factorization and sparse coding for functional brain overlapping community detection. *Cogn. Comput.*, 10(6):991–1005, 2018.
- [29] H. Liu, L. Liu, T. D. Le, I. Lee, S. Sun, and J. Li. Nonparametric sparse matrix decomposition for cross-view dimensionality reduction. *IEEE Trans. Multim.*, 19(8):1848–1859, 2017.
- [30] R. Luss and M. Teboulle. Conditional gradient algorithms for rank-one matrix approximations with a sparsity constraint. *SIAM Rev.*, 55(1):65–98, 2013.
- [31] A. Marmin, J. H. de Morais Goulart, and C. Févotte. Majorization-minimization for sparse nonnegative matrix factorization with the  $\beta$ -divergence. *IEEE Trans. Signal Process.*, 71:1435–1447, 2023.
- [32] A. Mazumdar and A. S. Rawat. Learning and recovery in the ReLU model. In *57th Annual Allerton Conference on Communication, Control, and Computing, Allerton 2019, Monticello, IL, USA, September 24-27, 2019*, pages 108–115. IEEE, 2019.
- [33] M. C. Mukkamala. *Bregman proximal minimization algorithms, analysis and applications*. PhD thesis, Universität Tübingen, 2022.
- [34] M. C. Mukkamala and P. Ochs. Beyond alternating updates for matrix factorization with inertial Bregman proximal gradient algorithms. In *Advances in Neural Information Processing Systems 32*, pages 4268–4278, 2019.
- [35] M. C. Mukkamala, P. Ochs, T. Pock, and S. Sabach. Convex-concave backtracking for inertial bregman proximal gradient algorithms in nonconvex optimization. *SIAM J. Math. Data Sci.*, 2(3):658–682, 2020.
- [36] Y. E. Nesterov. *Lectures on Convex Optimization*. Springer International Publishing, 2018.
- [37] D. N. Phan and H. A. Le Thi. Difference-of-convex algorithm with extrapolation for nonconvex, nonsmooth optimization problems. *Mathematics of Operations Research*, 49(3):1973–1985, 2024.
- [38] T. Pock and S. Sabach. Inertial proximal alternating linearized minimization (iPALM) for nonconvex and nonsmooth problems. *SIAM J. Imaging Sci.*, 9(4):1756–1787, 2016.
- [39] B. Recht, M. Fazel, and P. A. Parrilo. Guaranteed minimum-rank solutions of linear matrix equations via nuclear norm minimization. *SIAM Rev.*, 52(3):471–501, 2010.
- [40] R. Rockafellar and R.-B. Wets. *Variational Analysis*. Springer, 1998.
- [41] L. K. Saul. A nonlinear matrix decomposition for mining the zeros of sparse data. *SIAM J. Math. Data Sci.*, 4(2):431–463, 2022.
- [42] L. K. Saul. A geometrical connection between sparse and low-rank matrices and its application to manifold learning. *Trans. Mach. Learn. Res.*, pages 1–21, 2023.

- [43] G. Seraghihi, A. Awari, A. Vandaele, M. Porcelli, and N. Gillis. Accelerated algorithms for nonlinear matrix decomposition with the ReLU function. In *2023 IEEE 33rd International Workshop on Machine Learning for Signal Processing (MLSP)*, pages 1–6, 2023.
- [44] F. Shahnaz, M. W. Berry, V. P. Pauca, and R. J. Plemmons. Document clustering using nonnegative matrix factorization. *Inf. Process. Manag.*, 42(2):373–386, 2006.
- [45] S. Takahashi, M. Fukuda, and M. Tanaka. New bregman proximal type algorithms for solving DC optimization problems. *Comput. Optim. Appl.*, 83(3):893–931, 2022.
- [46] R. Tibshirani. Regression shrinkage and selection via the lasso. *J. R. Stat. Soc. Series B Stat. Methodol.*, 58(1):267–288, 1996.
- [47] M. Udell, C. Horn, R. Zadeh, and S. Boyd. Generalized low rank models. *Found. Trends Mach. Learn.*, 9(1):1–118, 2016.
- [48] D. Wang, T. Li, P. Deng, F. Zhang, W. Huang, P. Zhang, and J. Liu. A generalized deep learning clustering algorithm based on non-negative matrix factorization. *ACM Trans. Knowl. Discov. Data*, 17(7):99:1–99:20, 2023.
- [49] Q. Wang, C. Cui, and D. Han. A momentum accelerated algorithm for ReLU-based nonlinear matrix decomposition. *IEEE Signal Proc. Lett.*, 31:2865–2869, 2024.
- [50] Q. Wang and D. Han. A generalized inertial proximal alternating linearized minimization method for nonconvex nonsmooth problems. *Appl. Numer. Math.*, 189:66–87, 2023.
- [51] Q. Wang, D. Han, and W. Zhang. A customized inertial proximal alternating minimization for SVD-free robust principal component analysis. *Optimization*, 73(8):2387–2412, 2024.
- [52] Q. Wang, Z. Liu, C. Cui, and D. Han. A Bregman proximal stochastic gradient method with extrapolation for nonconvex nonsmooth problems. In *Proceedings of the AAAI Conference on Artificial Intelligence*, volume 38, pages 15580–15588, 2024.
- [53] J. Wright and Y. Ma. *High-Dimensional Data Analysis with Low-Dimensional Models: Principles, Computation, and Applications*. Cambridge University Press, Cambridge, 2022.
- [54] W. Wu, Y. Jia, S. Kwong, and J. Hou. Pairwise constraint propagation-induced symmetric nonnegative matrix factorization. *IEEE Trans. Neural Networks Learn. Syst.*, 29(12):6348–6361, 2018.
- [55] F. Xiong, J. Zhou, J. Lu, and Y. Qian. Nonconvex nonseparable sparse nonnegative matrix factorization for hyperspectral unmixing. *IEEE J. Sel. Top. Appl. Earth Obs. Remote. Sens.*, 13:6088–6100, 2020.
- [56] C.-H. Zhang. Nearly unbiased variable selection under minimax concave penalty. *Ann. Stat.*, 38(2):894–942, 2010.